land

MDPI

Article

Effects of Cropland Expansion on Temperature Extremes in Western India from 1982 to 2015

Jinxiu Liu [1], Weihao Shen [1] and Yaqian He [2,*]

[1] School of Information Engineering, China University of Geosciences, Beijing 100083, China; jinxiuliu@cugb.edu.cn (J.L.); 1004185223@cugb.edu.cn (W.S.)
[2] Department of Geography, University of Central Arkansas, Conway, AR 72035, USA
* Correspondence: yhe@uca.edu; Tel.: +1-304-777-3037

Abstract: India has experienced extensive land cover and land use change (LCLUC). However, there is still limited empirical research regarding the impact of LCLUC on climate extremes in India. Here, we applied statistical methods to assess how cropland expansion has influenced temperature extremes in India from 1982 to 2015 using a new land cover and land use dataset and ECMWF Reanalysis V5 (ERA5) climate data. Our results show that during the last 34 years, croplands in western India increased by ~33.7 percentage points. This cropland expansion shows a significantly negative impact on the maxima of daily maximum temperature (TXx), while its impacts on the maxima of daily minimum temperature and the minima of daily maximum and minimum temperature are limited. It is estimated that if cropland expansion had not taken place in western India over the 1982 to 2015 period, TXx would likely have increased by 0.74 (±0.64) °C. The negative impact of croplands on reducing the TXx extreme is likely due to evaporative cooling from intensified evapotranspiration associated with croplands, resulting in increased latent heat flux and decreased sensible heat flux. This study underscores the important influences of cropland expansion on temperature extremes and can be applicable to other geographic regions experiencing LCLUC.

Keywords: cropland expansion; climate extremes; western Indian; land cover and land use change; GLASS-GLC; maxima of daily maximum temperature

check for updates

Citation: Liu, J.; Shen, W.; He, Y. Effects of Cropland Expansion on Temperature Extremes in Western India from 1982 to 2015. *Land* **2021**, *10*, 489. https://doi.org/10.3390/land10050489

Academic Editor: Nir Krakauer

Received: 24 March 2021
Accepted: 1 May 2021
Published: 5 May 2021

Publisher's Note: MDPI stays neutral with regard to jurisdictional claims in published maps and institutional affiliations.

Copyright: © 2021 by the authors. Licensee MDPI, Basel, Switzerland. This article is an open access article distributed under the terms and conditions of the Creative Commons Attribution (CC BY) license (https://creativecommons.org/licenses/by/4.0/).

1. Introduction

Climate extremes, such as heat waves, droughts, and flooding, are among the most ecologically and economically significant hazards that affect millions of people globally [1]. India, located in South Asia (Figure 1), is one of the most populous countries and has experienced intensified climate extremes over the last four decades [2–4]. Between 1950 and 2015, central India has experienced a three-fold rise in extreme precipitation events [2], affecting the food and water security of the country's more than one billion people, especially the poor [5]. In 2010, India faced a severe heat wave, with temperatures reaching as high as 46.8 °C [6], resulting in the deaths of 269 people [7]. Such deadly consequences emphasize the importance of improving our understanding of the causes of climate extremes in India.

Among the factors driving climate extremes [8], greenhouse gas (GHG) emission-induced global warming is a first-order contributor [9,10]. Climate change can affect climate extremes through both dynamic (linked to the atmospheric circulation) and thermodynamic (linked to atmospheric water vapor content) processes [10]. However, climate change alone cannot completely explain the dynamics of climate extremes [11]. Another key factor influencing climate extremes is land cover and land use (LCLU) [12]. To date, approximately 41% of the Earth's surface has been changed, with natural vegetation such as forest and grassland replaced by other land cover and land use types such as cropland and built-up areas [13]. Such extensive LCLUC is likely to influence both weather and climate, as the land surface sets the prescribed conditions for the overlying atmosphere

through biogeophysical processes that affect soil moisture, energy balance, boundary layer development, and biogeochemical processes that alter carbon emission [14–18].

Considerable evidence indicates that LCLUC has affected regional climate in India [19–21]. More than 25% of the warming from 2001 to 2010 in the Eastern state of Odisha, India, was associated with urbanization [22]. This urbanization-induced warming also shows in other cities in India. From 2008 to 2016, the mean surface temperature in Surat and Bharuch has increased at a rate of 2.42 °C/decade and 2.13 °C/decade, respectively [23]. In contrast, Nayak and Mandal (2019) suggested that the conversion of shrubs to agricultural areas increased transpiration in India, contributing to a cooling by ~0.02 °C/decade during 1981 to 2006 [24]. The LCLUC also affects Indian rainfall patterns. Irrigation-induced evaporative cooling during the pre-monsoon season has caused decreased July surface temperature and a reduced land–sea thermal contrast, which has resulted in a weak summer monsoon in India [25]. A similar conclusion was revealed by a modeling study showing that deforestation in India resulted in decreasing evapotranspiration and subsequently decreased the recycled component of precipitation, leading to a weakening of the India summer monsoon [26].

While the impacts of LCLUC on mean climate in India have been widely explored, LCLUC is rarely studied as a causing factor for climate extremes [12]. However, recently, several modeling studies have claimed that LCLUC could influence climate extremes [14,27,28]. Sy and Quesada (2020) used five Earth system models to identify LCLUC impacts on 20 extreme weather indices over the 21st century. They found that in Southern Asia, LCLUC can lessen projections of very wet days (annual total precipitation from days >95th percentile) by 38%, and enhance projection of the annual maxima of daily maximum temperature by 1.11% [29]. Nevertheless, such model-based studies have produced inconsistent results. For instance, Christidis et al. (2013) found that daily temperature extremes are less severe with deforestation [30], while Strack et al. (2008) claimed the enhanced severity of June extremes [31]. This spread of model response in extreme climates is presumably due to the fact that the models differ in terms of their dynamical cores, numerical schemes, parameterizations, and simulation periods [16,32]. In addition, most modeling studies employed extreme sensitivity experiments by completely replacing one land cover and land use type with another type (e.g., replacing forests with bare ground for deforestation experiments). Such extreme experiments are likely to be unrealistic, as regional vegetation changes are usually gradual, and rarely involve total change to an entire landscape [33]. Therefore, observational studies are critical to confirm the model results and quantify the real-world LCLUC impacts on climate extremes.

We address some of these aforementioned limitations by using novel 34-year land cover and land use data derived from satellite data to empirically quantify cropland expansion effects on temperature extremes in India. As one of the first attempts, this study aims to address the following questions: (1) What are the spatiotemporal patterns of croplands in India during the last three decades? (2) How does cropland expansion in India affect temperature extremes? and (3) What are the physical mechanisms underlying the influences?

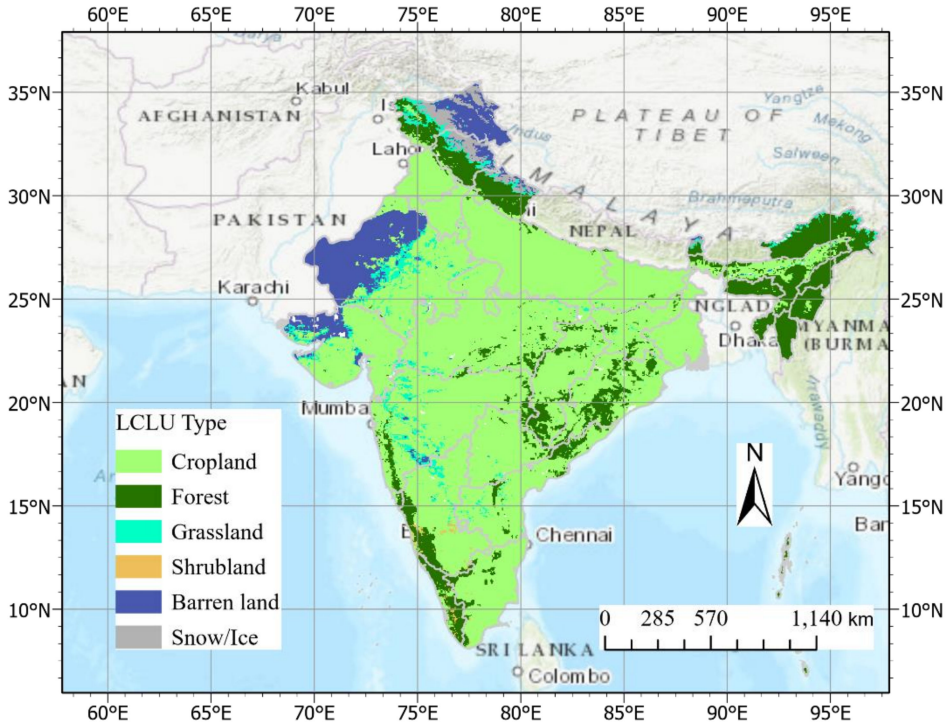

Figure 1. Study area of India with the land cover and land use information in the year 2015 from the Global Land Surface Satellite global land cover (GLASS-GLC) dataset [34] (The map is made using ArcGIS Pro 2.8 with geographic coordinate system of WGS 1984, angular unit of Degree, prime meridian of Greenwich, datum of D_WGS_1984, spheroid of WGS 1984, semimajor axis of 6378137.0, semiminor axis of 6356752.3, and inverse flattening of 298.3).

2. Materials and Methods

2.1. Materials

The land cover and land use data used in this study is the Global Land Surface Satellite Global Land Cover (GLASS-GLC) dataset downloaded from https://doi.pangaea.de/10.1594/PANGAEA.913496 (accessed on 23 March 2021) [34]. This newly released annual-scale LCLU data from 1982 to 2015 was generated using a random forest classifier based on multisource remotely sensed datasets, including a normalized difference vegetation index (NDVI), leaf area index (LAI) and fraction of absorbed photosynthetically active radiation (FAPAR) from GLASS climate data records (CDRs), and elevation data from Global Multi-resolution Terrain Elevation Data 2010 (GMTED2010) [34]. Based on a comparison with more than 2000 reference samples, the overall accuracy of the GLASS-GLC dataset was estimated at ~82.81%, which is higher than that of the widely used Moderate Resolution Imaging Spectroradiometer (MODIS) land cover product (~73.9%) and the European Space Agency Climate Change Initiative (ESA-CCI) land cover data (~80.38%) [34]. The spatial resolution of GLASS-GLC data is 5 km with seven classes: cropland, forest, grassland, shrubland, tundra, barren land, and snow/ice. We use the "raster" package in R [35] to extract the GLASS-GLC for India (Figure 1). To be consistent with the meteorological data described below, we aggregate the 34-year LCLU maps from 5 km to 0.25° over 1982 to 2015 using a fractional method following He et al. [33], to generate maps of the fraction of the area in India covered by cropland for each year.

The temperature data is obtained from European Center for Medium-Range Weather Forecasts (ECMWF) Reanalysis 5th Generation (ERA5) (https://cds.climate.copernicus.eu/cdsapp#!/dataset/reanalysis-era5-single-levels?tab=form (accessed on 23 March 2021)) [36]. ERA5 assimilates a combination of historical observations, including both satellite and in situ data into global estimates [36]. Compared to the prior release of this dataset, ERA-Interim, there were numerous enhancements and advances in ERA5 [36]. In particular, the

spatial resolution was improved from ~0.7° to 0.25° for atmospheric variables and 0.1° for land variables, and the temporal coverage was extended back to 1950. ERA5 provides hourly data for a large number of atmospheric, ocean-wave, and land surface variables [36]. In this study, we used the hourly maximum and minimum 2 m temperature in ERA5 from 1982 to 2015, to be consistent with the LCLU data time period. We then calculated the daily maximum and minimum and annual temperature extremes from the hourly data. The metrics included TXx (defined as the maxima of daily maximum temperature values) (the warmest day), TXn (referring to the minima of daily maximum temperature) (the coldest day), TNx (the maxima of daily minimum temperature) (the warmest night), and TNn (the minima of daily minimum temperature) (the coldest night). To explore the associated physical mechanism, we also obtain the monthly evapotranspiration from bare soil, evaporation from open water surface excluding oceans, and evaporation from vegetation transpiration to calculate the monthly total evapotranspiration. We also acquired the surface latent and sensible heat fluxes. The mean summer (JJA: June, July, and August) evapotranspiration, and latent and sensible heat fluxes are then calculated for each year from 1982 to 2015.

2.2. Methods

The flowchart of methods is shown in Figure 2. Based on cropland fraction data from 1982 to 2015, we first used trend analysis to determine the regions with significantly increased croplands and the regions without significantly changed croplands. Then, correlation analysis and Welch's mean test were applied to explore the relationships between cropland fraction and temperature extremes. To investigate the magnitude of cropland expansion on temperature extremes, this study used linear regression analysis. Finally, we applied a composite analysis based on evapotranspiration, latent heat flux, and sensible heat flux data to examine the possible physical mechanism underlying the empirical impacts of cropland expansion on temperature extremes. The description of each statistical method is presented in the following.

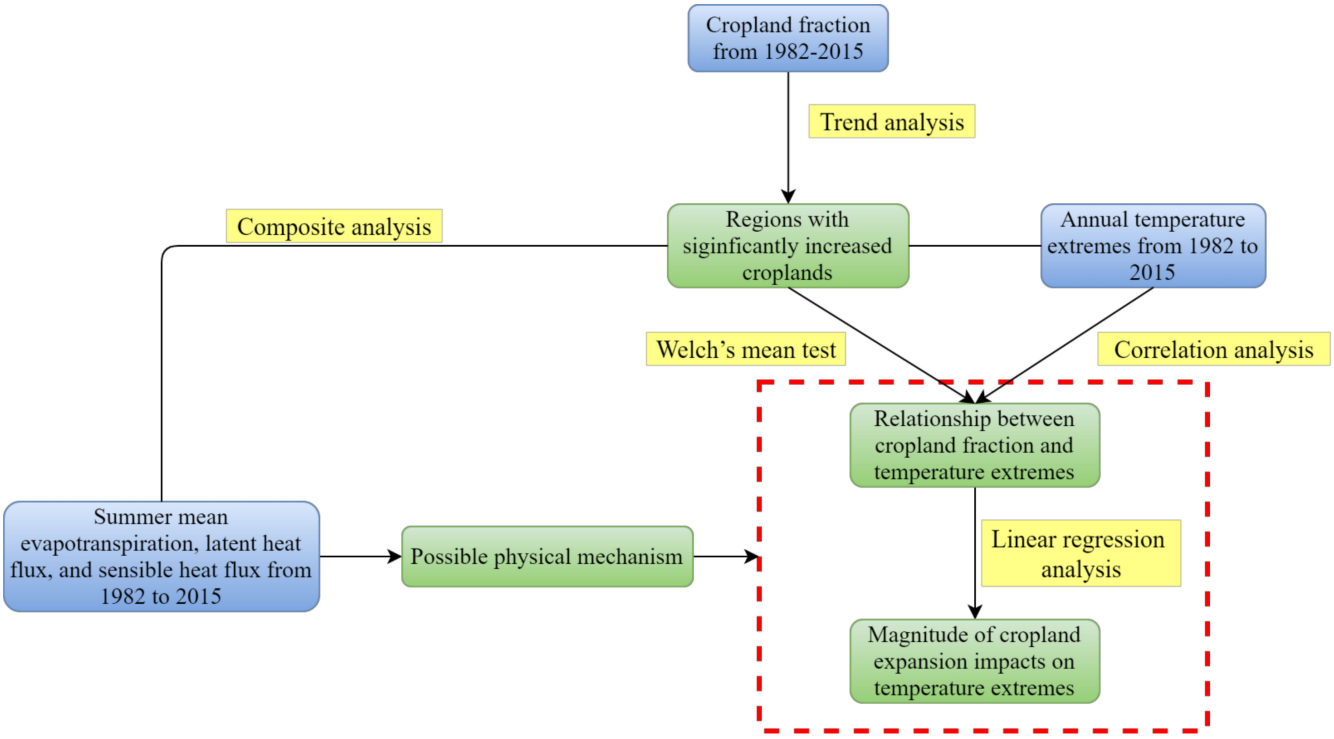

Figure 2. Flowchart of methods (blue color is for input, green color is for output, and yellow color is for statistical methods).

2.2.1. Autocorrelation-Adjusted Trend Analysis

To investigate the spatiotemporal changes of croplands in India, for each grid point, we regressed the cropland fraction on time with an autocorrelation-corrected linear fit. Correction for temporal autocorrelation is necessary, because autocorrelation can lead to an overestimate of statistical significance in temporal linear trends [18,37]. The time series of cropland fraction was first fit with an ordinary least squares (OLS) regression, then the residuals of this OLS coefficient were tested for autocorrelation. If autocorrelation was significant at the 5% level, we fitted a generalized least squares (GLS) regression estimated using an autoregressive moving average process of order p = 1 or p = 2, based on the data's covariance structure. The significance of the trend was tested by a Student's *t* test.

2.2.2. Correlation Analysis and Welch's Mean Test

We used non-parametric Spearman's correlation analysis to examine relationships between the cropland fraction and the climatic variables, including the annual maxima and minima of daily maximum and minimum temperature. The cropland fraction and climatic variables were averaged over the region in western India with significantly increasing croplands. The region is indicated as the dashed rectangle in Figure 3b (see the discussion in Section 3.1.). We chose this region because it is likely to be most associated with the regional climate signal we assessed [18,38,39]. The linear trends in the area-averaged cropland fraction and climate extremes were removed to isolate global warming impacts following previous studies (e.g., [40]). The significance of the correlation was tested with Student's *t* test.

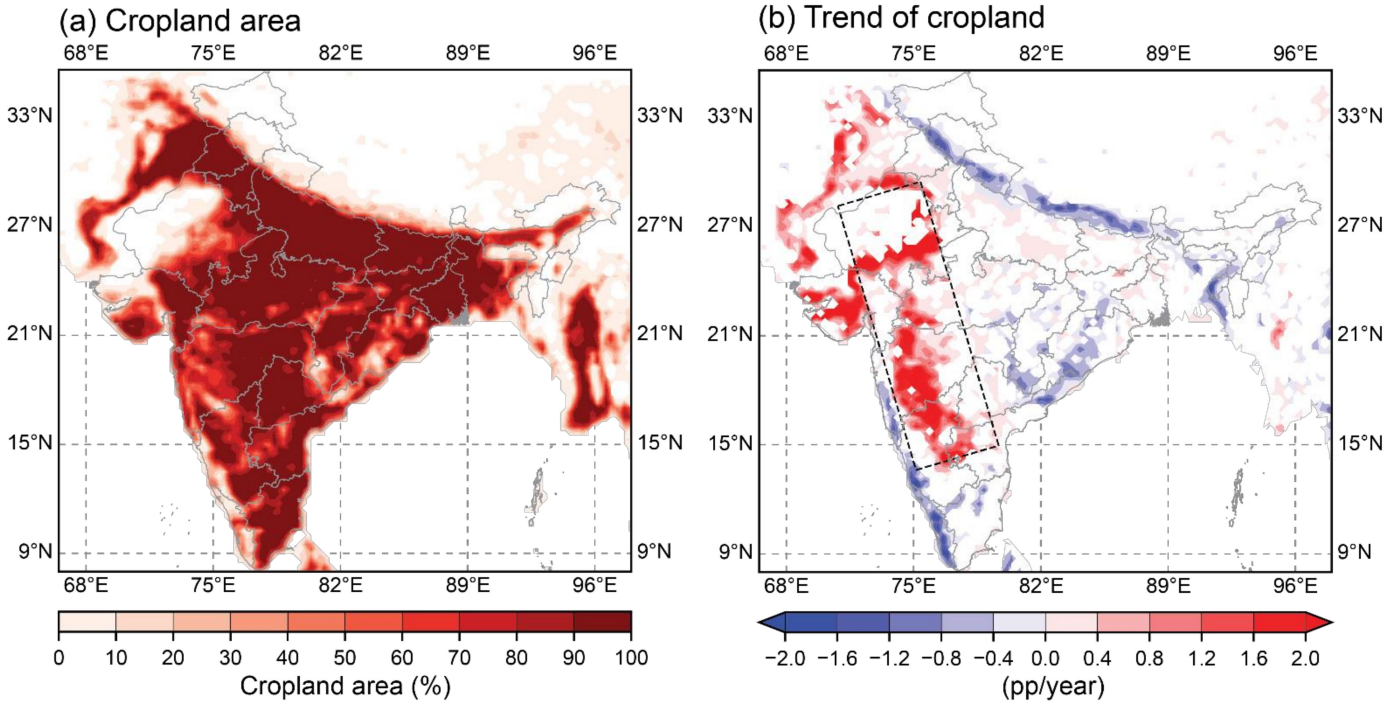

Figure 3. (**a**) Mean fraction of cropland area for India from 1982 to 2015 (the color bar is the percentage of cropland in each 0.25° grid cell) and (**b**) significant (*p*-value < 0.1) trends in cropland fraction estimated from 1982 to 2015 (the color bar in **(b)** is the slope in percentage points (pp) per year). The dashed rectangle in (**b**) denotes western India, the focus area of this study.

To confirm the correlation analysis, we also compared the mean temperature extremes of the regions with significantly increased croplands with that of regions without significantly changed croplands using Welch's *t* test. Welch's *t* test is a modification of the Student's *t* test that can take into account the variations in sample sizes and variances [41]. Because the number of grid cells falling within regions with significantly increased crop-

lands and areas without significantly-changed croplands is unequal, we therefore chose a Welch's *t* test [41]

2.2.3. Linear Regression Analysis

To quantify the magnitude of cropland expansion impacts on climate extremes in the regions with significantly increased croplands, we first regressed climate extremes (i.e., TXx, TXn, TNx, and TNn) on the cropland fraction using univariate linear regression. The independent variable was the area-averaged detrended cropland fraction of all grid cells within the regions with significantly increased croplands and the area-averaged and detrended climate extremes over the same grid points were used as dependent variables in the univariate regression. We then multiplied the magnitudes of cropland impacts on different climate extremes with the regression coefficients of cropland expansion, calculated from the OLS linear trend for the 34-year cropland values, to estimate the counterfactual climate extremes that would have occurred if cropland expansion had not taken place.

2.2.4. Composite Analysis

We performed composite difference analysis to explore possible physical mechanisms relating cropland expansion to climatic variables. Composite difference analysis is a sampling technique based on the conditional probability of the occurrence of a particular event [42]. We conducted composite analysis based on eight years with detrended area-averaged cropland fractions above ~75th percentile as the conditional event. Composite differences of latent and sensible heat fluxes for each grid cell were calculated by subtracting the mean value for those eight years from the climatological mean value over the 34 years of the study period. The significance for the composite difference was also estimated using a Welch's *t* test.

3. Results and Discussion

3.1. Cropland Expansion in Western India

The main LCLU types in India are cropland, forest, grassland, shrubland, and barren land (Figure 1). Croplands are generally dominant across India, comprising more than 40% of land cover for most areas, except peripheral regions, especially the northwestern barren regions (Figure 3a). Croplands in India showed notable spatial and temporal changes from 1982 to 2015. Croplands significantly increased in western India and the surrounding areas of the northwestern barren lands, with an increase of up to 2 percentage points (pp) per year (Figure 3b). This trend of increasing croplands in western India is largely consistent with previous studies. Roy et al. (2015) used spatial resolution Landsat images for three epochs (1985, 1995, and 2005) to detect LCLUC, and found croplands increased in Maharashtra and Madhya Pradesh, western India [43]. Using the same satellite data, a study identified several hotspots of agricultural lands expansion in the Mula-Pravara basin in western India from 1991 to 2016 [44]. Grasslands, on the other hand, significantly decreased in this region, while forest and shrubland did not change significantly (Figure A1, see Appendix A). This indicates that the significant increase of croplands in western India is largely due to decreasing grasslands, which may be attributed in part to an increase in human population since the 1980s [45]. It may also be associated with improved access to water resources and increased road networks as a result of government promotional schemes (e.g., National Horticulture Mission initiated in 2005) that provide subsidies, technical support, and capacity-building activities to promote commercial crop development in India [44,46].

We area-averaged the cropland fraction over the grid cells with significantly increasing cropland in western India (Figure 4, yellow–green line). The area-averaged cropland fraction increased significantly by ~0.99 ($\pm$0.109) pp per year (p-value < 0.01), a total of ~33.7 pp increase during the 34 years studied. Such a vast and rapid expansion of croplands in western India has the potential to alter the water and energy balance in the boundary layer, affecting mean climatology and extremes. Therefore, in the following

analyses, we focused on the region indicated as the dashed rectangle in western India (Figure 3b) to cover the majority of grid cells that experienced significantly increased croplands to investigate the effects of cropland expansion on temperature extremes and possible associated physical mechanisms.

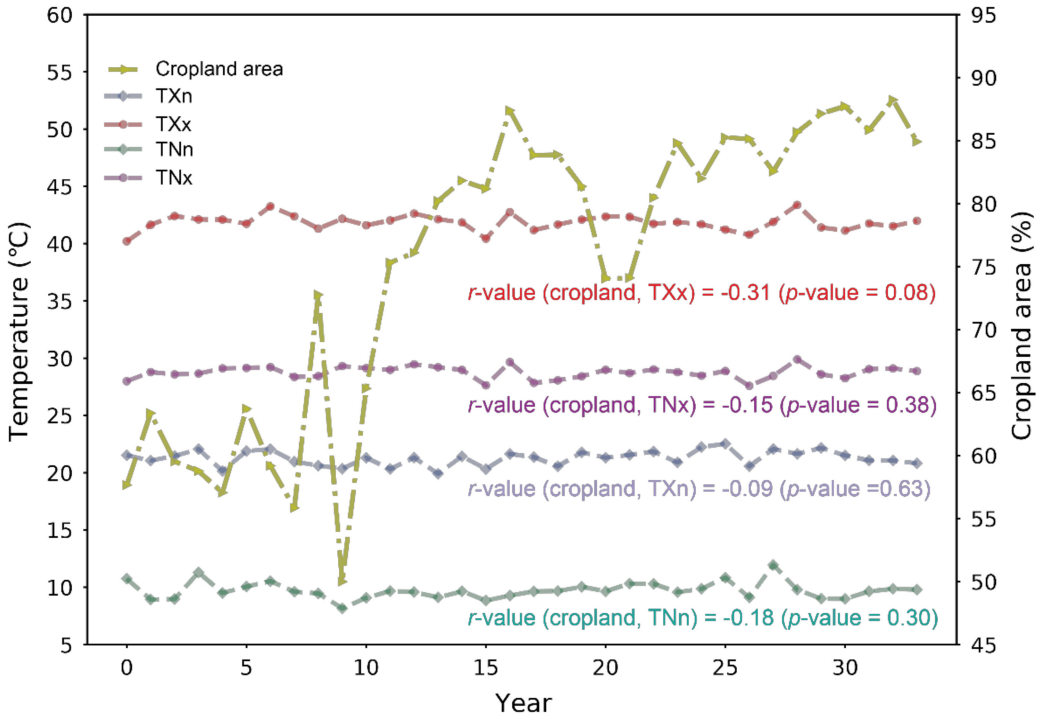

Figure 4. Time series of annual cropland fraction (yellow–green line), maxima of daily maximum temperature (TXx, red line), minima of daily maximum temperature (TXn, blue line), maxima of daily minimum temperature (TNx, purple line), and minima of daily minimum temperature (TNn, green line), averaged over regions with significantly increasing croplands from 1982 to 2015 in western India. The values denote Spearman's correlations of the detrended area-averaged cropland fraction with detrended TXx (red), TXn (blue), TNx (purple), and TNn (green), respectively.

3.2. Impacts of Cropland Expansion on Temperature Extremes in Western India

To explore the empirical relationships between cropland fraction and temperature extremes within the focus of western India, we conducted a correlation analysis of the detrended area-averaged cropland fraction with the detrended area-averaged maxima of daily maximum temperature (Figure 4, red line), the minima of daily maximum temperature (Figure 4, blue line), the maximum of daily minimum temperature (Figure 4, purple line), and the minima of daily minimum temperature (Figure 4, green line). The results show a significantly negative correlation (r-value = −0.31) between cropland fraction and TXx (Figure 4), indicating that in areas where cropland fraction increased, TXx decreased. A negative correlation of cropland expansion with TXx is also identified by a prior modeling study. It used the Community Earth System Model (CESM) to assess the roles of LCLUC on temperature extremes, and found that global TXx decreased by 0.22 K because of increasing croplands [27]. Similarly, Thiery et al. (2017) stated that due to increasing croplands-related irrigation, TXx decreased by 0.78 K over global irrigated land [47]. The correlations between cropland area and TXn, TNx, and TNn were also negative; however, they were non-significant (p-value = 0.63, 0.38, 0.30, respectively) (Figure 4). The lesser impacts of cropland fraction on TNn in India are in conformity with Thiery et al. (2017), who reported that irrigation-induced TNn cooling was much smaller compared to TXx in southern Asia [47], while Niu et al. (2019) pointed out that cropland expansion had stronger effects on TNn and TNx compared to TXx and TXn in India [48]. This indicates that in western India, the effects of cropland area on the minima of daily maximum temperature

and the maxima and minima of daily minimum temperature need to be further explored. In the following analyses, we therefore focused on TXx.

To confirm the significantly negative correlation between cropland area and TXx, we conducted Welch's mean test to test whether in western India the mean non-detrended TXx over the regions with significantly increasing croplands was significantly smaller than that over the regions with non-significantly changed croplands. We assumed that if the negative correlation were robust, TXx would show a decrease over the regions with significantly increasing croplands compared to that over the regions with non-significantly changed croplands. The results show that the mean maxima of daily maximum temperature over the regions with significantly increased croplands was ~41.8 °C, while the TXx over the regions without significantly changed croplands was ~42.8 °C (Figure 5). The difference of −1.0 °C in mean TXx was significant (p-value < 0.1) (Figure 5), indicating that cropland area does have a negative impact on the maxima of daily maximum temperature in western India, which confirms the aforementioned correlation analysis. This negative impact of cropland area on TXx is further confirmed by the smaller trend value of TXx over regions with significantly increased croplands (−0.0052 °C/year) compared to that over regions without significantly changed croplands (−0.0048 °C/year) (Figure A2a).

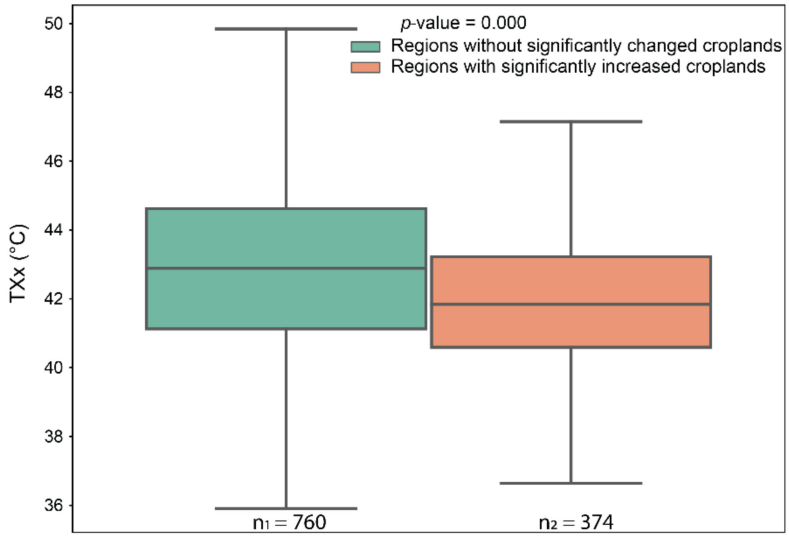

Figure 5. Welch's mean test for maxima of daily maximum temperature (TXx) over regions with significantly increasing croplands (right box) and that over regions without significantly changed croplands (left box). The n_1 and n_2 indicate the number of grid cells with significantly increased croplands and without significantly changed croplands, respectively.

We also conducted Welch's test for TXn, TNx, and TNn. (Figure A3). The lower TNx over the regions with significantly increasing croplands compared to that over the regions without significantly changed croplands denotes a negative impact of cropland area on TNx (Figure A3b), which is consistent with the correlation analysis (Figure 4) and the smaller trend value of TNx over regions with significantly increased croplands (−0.0009 °C/year) compared to that over regions without significantly changed croplands (0.0012 °C/year) (Figure A2c). However, in contrast to the correlation analysis, the results show that cropland area had a positive impact on the minima of daily maximum and minimum temperature (Figure A3a,c), although the smaller trend values of TXn and TNn over regions with significantly increased croplands (0.0115 °C/year and 0.0051 °C/year, respectively) compared to that over regions without significantly changed croplands (0.0146 °C/year and 0.0066 °C/year, respectively) were observed (Figure A2b,d). These discrepancies indicate that other factors (e.g., topography or other meteorological factors) may have impacts on TXn and TNn in western India [49,50]. For instance, Mishra et al. (2018) demonstrated that the improved representation of surface topography could enhance surface temperature

simulation in India [51]. Chowdary et al. (2014) found that temperature across India was influenced remotely by the El Niño Southern Oscillation. The EI Niño-induced strong subsidence, weaker low-level winds, less moisture variability, and enhanced incoming shortwave radiation over the north India Ocean and Indian subcontinent were responsible for summer air-temperature warming. Meanwhile, the temperature variability in India was also affected locally through the Indian Ocean's sea surface temperature (SST) [50]. During the fall, temperature in India was highly correlated with SST in north India ocean. In addition to oceanic influence, Kalsi and Pareek (2001) reported that the maximum temperature in India could be influenced by local anomalous circulation setting over India and its neighbors. In 1999, a negative field of divergence at 200 hpa over the Persian Gulf, Middle East countries, and the Indo-Pak region suppressed the convective activity that normally moderates the temperature field, leading to exceptional warming in India [52].

We used univariate linear regression to quantify the magnitude of cropland area impacts on TXx. Figure 6 shows that for each 1.0 percentage point increase in cropland area, TXx decreased by 0.022 (±0.019) °C. This further confirms our previous conclusion that cropland area has a negative impact on TXx, although the slope is not significant (p-value = 0.259). Nevertheless, by multiplying the slope with the cropland expansion values rate (i.e., ~0.99 (±0.109) pp/year), the counterfactual TXx indicates an increase of 0.74 (±0.64) °C if cropland expansion had not taken place in western India over the 1982 to 2015 period. The linear regression coefficients for TXn, TNx, and TNn were −0.006 (±0.019) °C/%, −0.012 (±0.015) °C/%, −0.007 (±0.021) °C/%, respectively (Figure A4), implying that cropland area also has a negative impact on these extremes; however, these relationships are not significant at the 10% level.

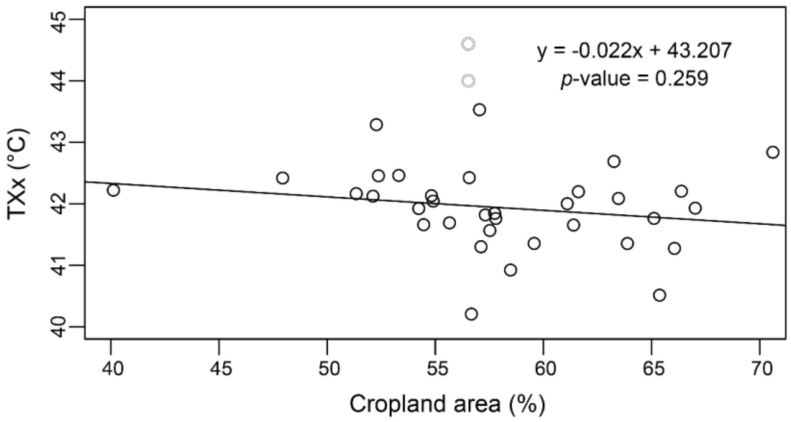

Figure 6. Linear association of detrended cropland fraction with detrended maxima of daily maximum temperature in western India, averaged over the regions with significantly increasing croplands from 1982 to 2015.

3.3. Possible Physical Mechanisms

To explore the underlying physical mechanism of cropland area impacts on hot extremes (i.e., TXx), we conducted a composite analysis for summer (JJA). We calculated the composite mean difference for evapotranspiration, latent heat flux, and sensible heat flux between eight years (1998, 1996, 1995, 1999, 1997, 2000, 1990, and 1993) with high detrended area-averaged cropland area (as described in the Methods Section) in western India and 34 years of the study period (Figure 7). The results show that during the years with a larger cropland area in western India, evapotranspiration was greater, compared to the climatology mean (Figure 7a). This difference was even stronger in the central part of the region, with more than 5 mm/month (Figure 7a), which was statistically significant. Croplands evaporate more efficiently compared to grasslands, especially during the summer when crops reach the peak growing period [53]. In addition, irrigation associated with croplands in western India [54] also contributed to the higher evapotranspiration. Higher evapotranspiration led to higher latent heat flux during the years with high cropland area

with more latent heat flux in the central region (Figure 7b). Correspondingly, sensible heat flux has decreased in western India (Figure 7c), although the significance has declined. The increasing latent heat flux and decreasing sensible heat flux due to cropland expansion and the associated agricultural activities (e.g., irrigation) have been supported by previous studies [27,47,55,56]. Ray et al. (2003) revealed that latent heat flux during the winter growing season over cropped areas was elevated compared to neighboring natural vegetation over the wheat lands of Western Australia [57]. Marcella and Eltahir (2014) also observed an increase of latent heat flux over the crop fields [58]. More recently, He et al. (2020) found that cropland expansion in northeastern China increased latent heat flux and decreased sensible heat flux [18].

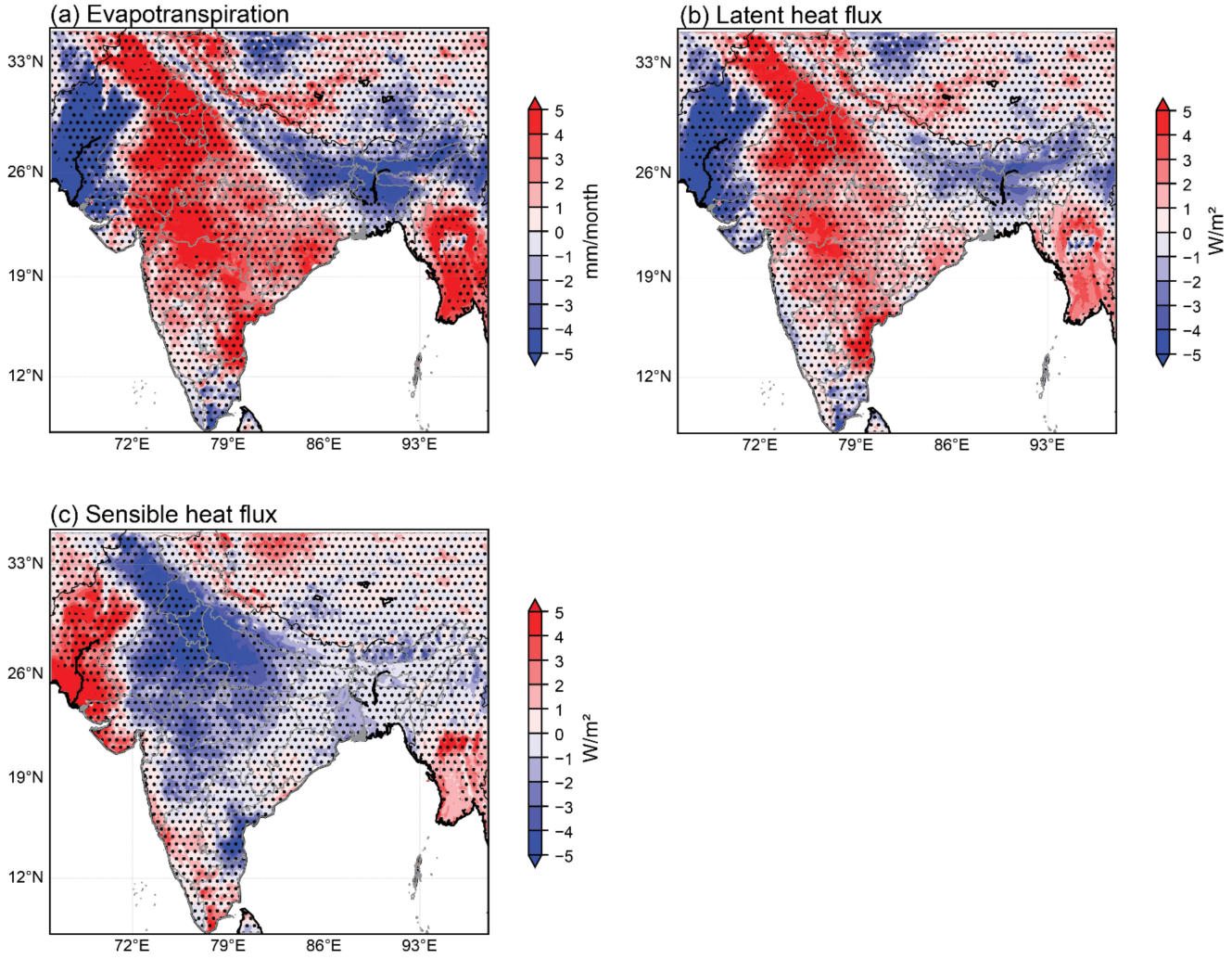

Figure 7. Composite difference patterns for (**a**) evapotranspiration, (**b**) latent heat flux, and (**c**) sensible heat flux between eight high-cropland years (1998, 1996, 1995, 1999, 1997, 2000, 1990, and 1993) based on detrended area-averaged cropland fraction over the 34 years of the study period at each grid cell during JJA. The un-stippled regions indicate a significant difference at the 10% level.

The generally consistent spatial patterns of evapotranspiration, latent heat flux, and sensible heat flux indicate that increased cropland area in western India could lead to more water vapor transpiration into the atmosphere, which results in more energy released as latent heat flux, subsequently reducing sensible heat flux, thus decreasing temperature (e.g., TXx). Figure 8 summarizes the possible physical mechanism. The data and method used in this study are applicable to other geographic regions, where land use and land cover change is ongoing.

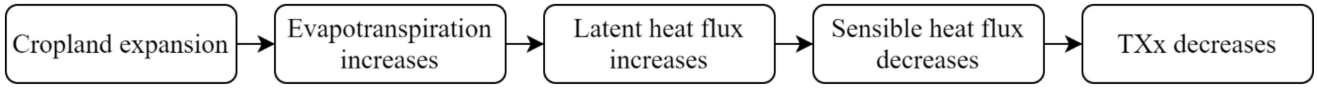

Figure 8. Possible physical mechanism.

4. Conclusions

Cropland expansion is one of the most important land cover and land use changes and has affected mean climate. However, how it influences climate extremes remains an open question in India. This study applied a newly developed land cover and land use dataset to empirically explore the impacts of cropland expansion in western India from 1982 to 2015 on temperature extremes, including the maxima of daily maximum and minimum temperature and the minima of daily maximum and minimum temperature.

We found that croplands significantly increased in western India spatiotemporally, with an increasing rate of ~0.99 pp per year during the last three decades. This extensive cropland expansion has a statistically negative impact on the maxima of daily maximum temperature. If cropland expansion had not taken place in western India over the 1982 to 2015 period, the maxima of daily maximum temperature would have increased by 0.74 ($\pm$0.64) °C, although it was not significant at the 10% level. This observational evidence underscores the important effects of cropland expansion on temperature extremes, which provides a scientific basis for policy makers to establish feasible agricultural land planning.

While our study addresses some limitations of prior studies regarding regional climate variability in India, there are several uncertainties in our findings that we plan to address in future work. First, we conducted Welch's mean test over regions with significantly increased croplands and non-significantly changed croplands. However, the background temperature over these regions could be different. Matching methods [59] that consider the base temperature information might solve this issue. Second, since topography affects climate, the elevation effects should be investigated. Third, although He et al. (2020) claimed that in northeastern China, the associations between cropland area and climatic variables could be seen both in the regions with significantly increased croplands and areas where croplands are present [18], the relationships identified in this study should be further explored in the regions with non-significant changed croplands due to the different geographic regions. Finally, considering the unique locations of India surrounded by the Arabian Sea and the Bay of Bengal, the climate of India could be influenced by oceanic forcings, such as SST [50], in addition to the changes of LCLU studied in this paper. Thus, other possible physical mechanisms related to oceanic forcing remain to be further explored.

Author Contributions: Conceptualization, Y.H.; methodology, J.L. and Y.H.; formal analysis, J.L., W.S., and Y.H.; data curation, J.L., W.S., and Y.H.; writing—original draft preparation, J.L. and Y.H.; writing—review and editing, J.L., W.S., and Y.H.; visualization, J.L., W.S., and Y.H.; supervision, J.L. and Y.H. All authors have read and agreed to the published version of the manuscript.

Funding: This research was supported by the Fundamental Research Funds for the Central Universities (grant number 2652018077).

Data Availability Statement: The ERA5 climate data is available through https://cds.climate.copernicus.eu/cdsapp#!/dataset/reanalysis-era5-pressure-levels?tab=overview and the GLASS-GLC data is downloaded from https://doi.pangaea.de/10.1594/PANGAEA.913496 (accessed on 23 March 2021).

Acknowledgments: We acknowledge European Centre for Medium-Range Weather Forecasts (ECMWF) for supporting ERA5 climate data and Peng Gong and Jie Wang from Tsinghua University, China for providing the GLASS-GLC dataset. We thank Timothy Warner from the Department of Geology and Geography at West Virginia University for improving the manuscript. We are also grateful to three anonymous reviewers and the academic editor for their constructive comments, which greatly strengthened this manuscript.

Conflicts of Interest: The authors declare no conflict of interest.

Appendix A

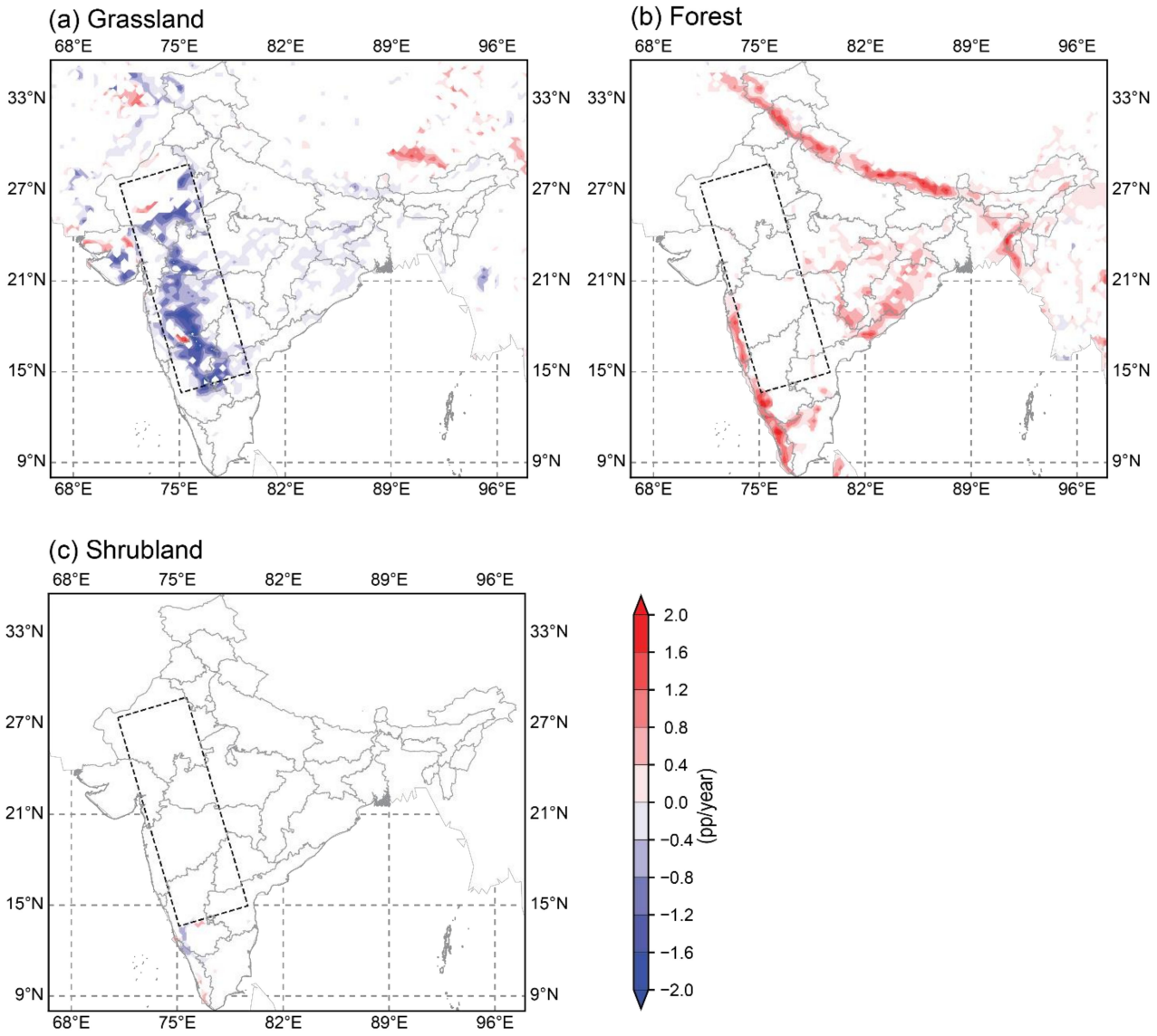

Figure A1. Significant (p-value < 0.1) trends in (**a**) grassland fraction, (**b**) forest fraction, and (**c**) shrubland fraction, estimated from 1982 to 2015 (the color bar is the slope in percentage points (pp) per year).

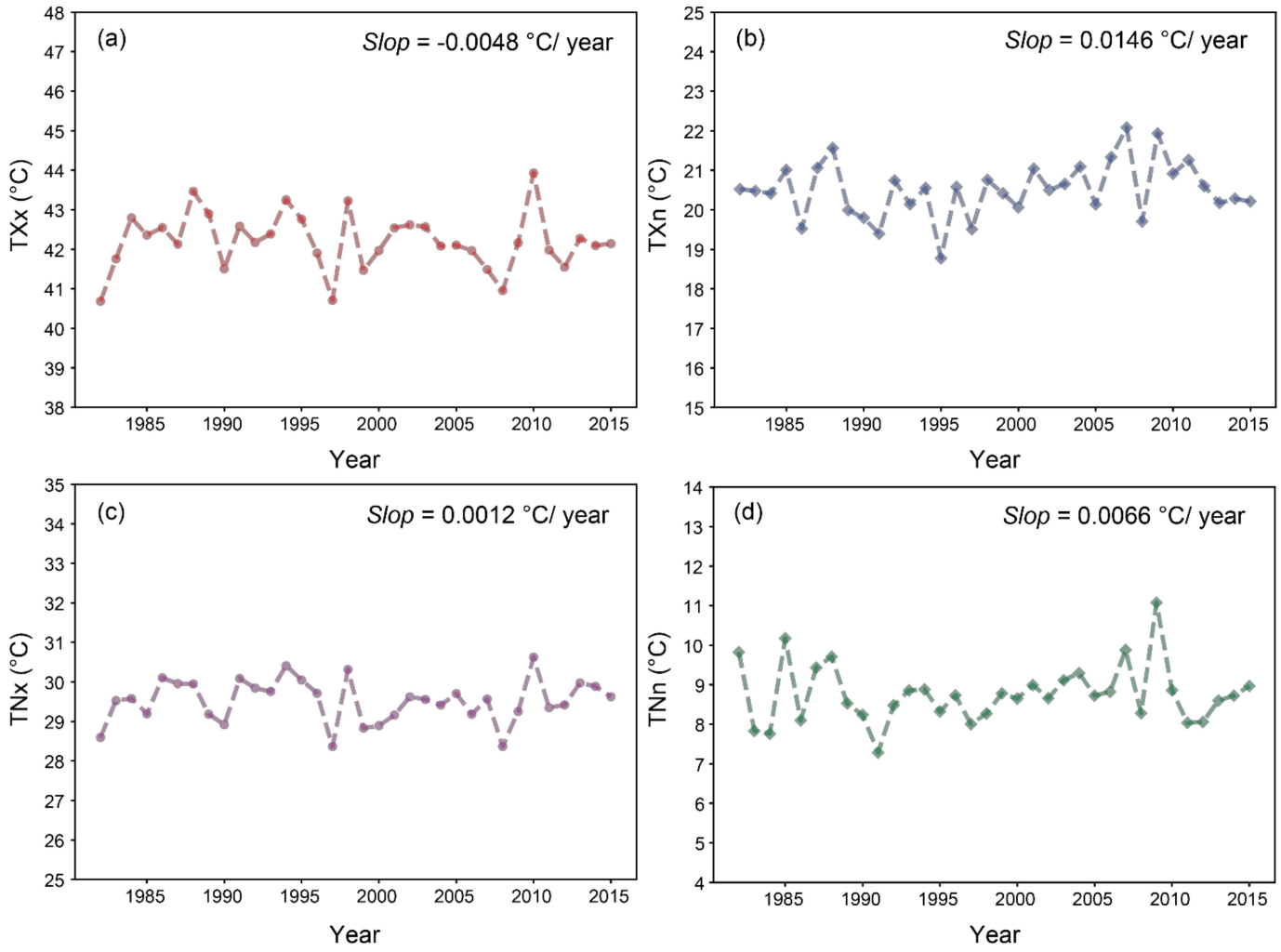

Figure A2. Time series of (**a**) maxima of daily maximum temperature (TXx), (**b**) minima of daily maximum temperature (TXn), (**c**) maxima of daily minimum temperature (TNx), and (**d**) minima of daily minimum temperature (TNn), over regions without significantly changed croplands in western India. The slope values are from the linear regression analysis.

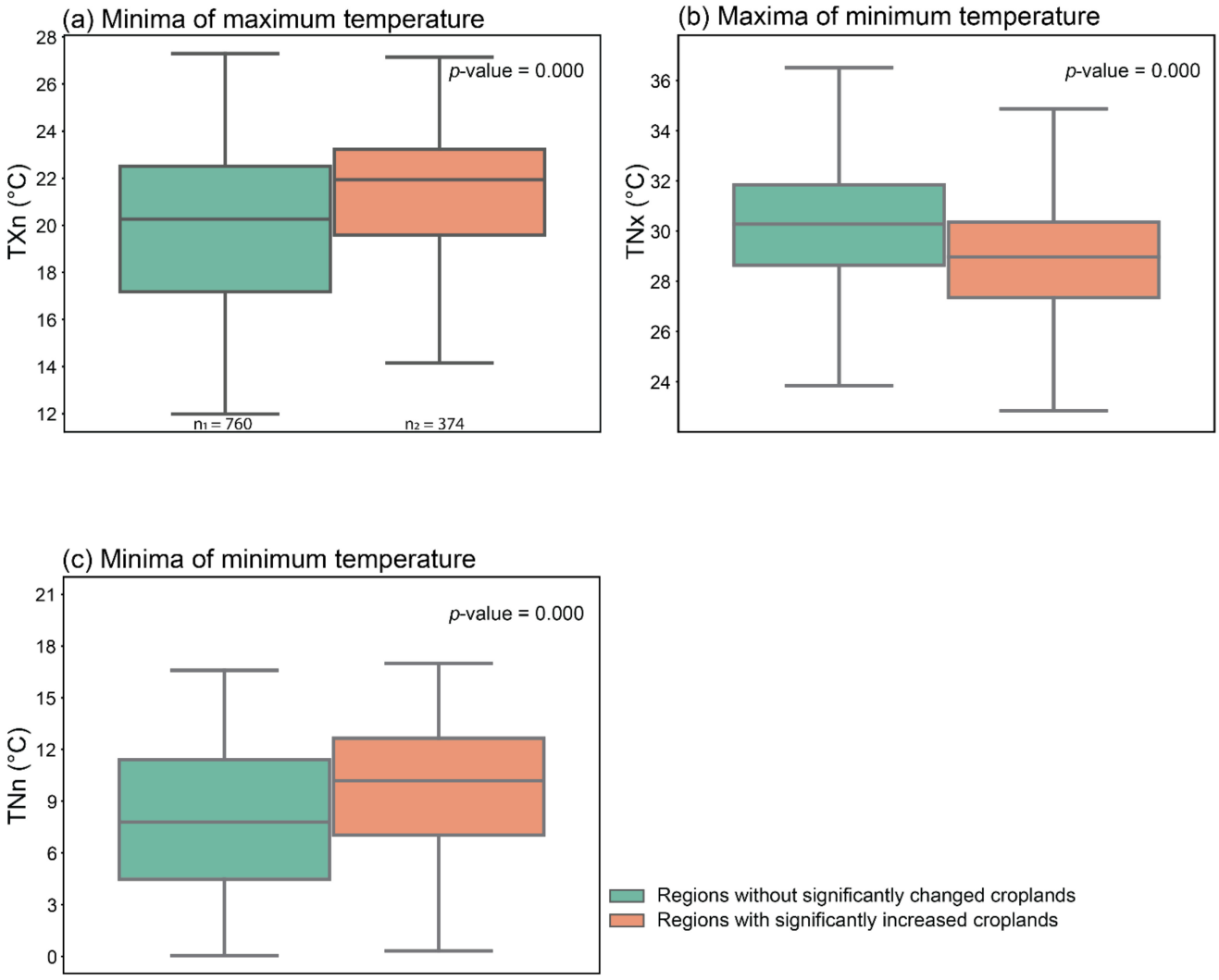

Figure A3. Welch's mean test for (**a**) minima of daily maximum temperature (TXn), (**b**) maxima of daily minimum temperature (TNx), and (**c**) minima of daily minimum temperature (TNn), over regions with significantly increasing croplands (right box) and that over regions without significantly changed croplands (left box). The n_1 and n_2 indicate the number of grid cells with significantly increased croplands and without significantly changed croplands, respectively.

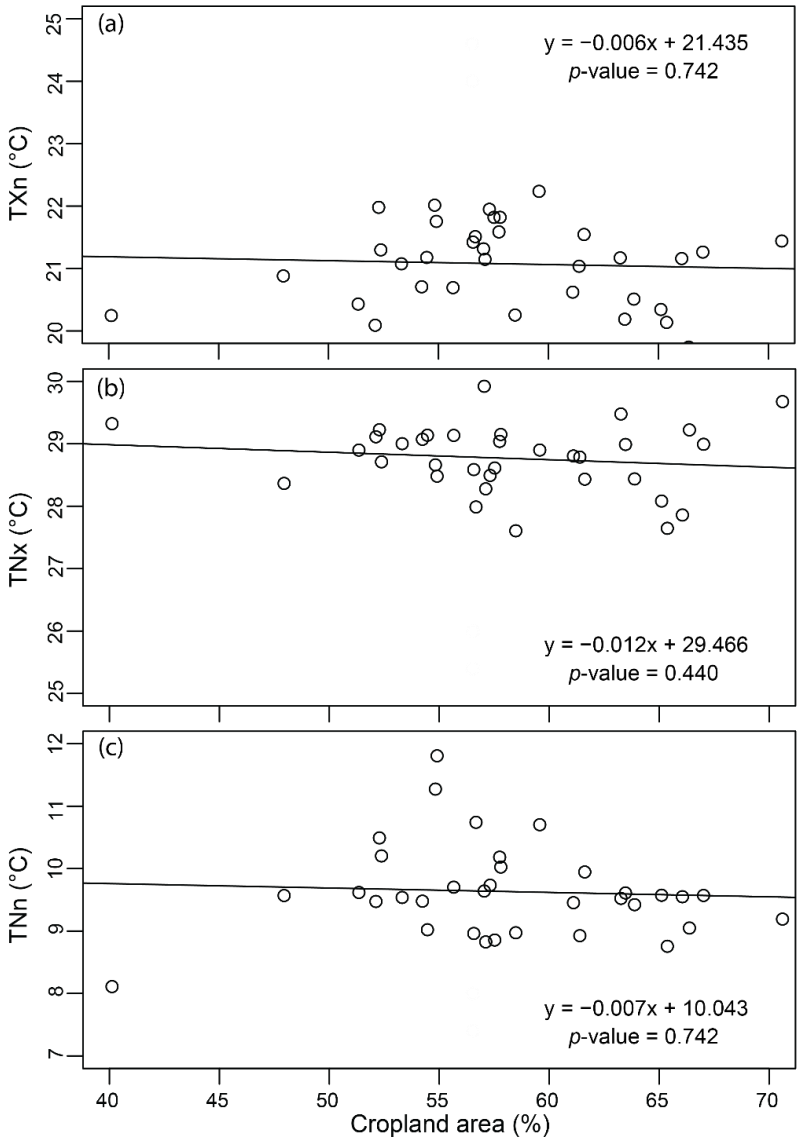

Figure A4. Linear association of detrended cropland fraction with detrended (**a**) minima of daily maximum temperature (TXn), (**b**) maxima of daily minimum temperature (TNx), and (**c**) minima of daily minimum temperature (TNn) in western India, averaged over the regions with significantly increasing croplands in western India from 1982 to 2015.

References

1. Liu, M.; Xu, X.; Xu, C.; Sun, A.Y.; Wang, K.; Scandon, B.R.; Zhang, L. Water Resources Research: Preface. *Water Resour. Res.* **2017**, *53*, 3262–3278. [CrossRef]
2. Roxy, M.K.; Ghosh, S.; Pathak, A.; Athulya, R.; Mujumdar, M.; Murtugudde, R.; Terray, P.; Rajeevan, M. A threefold rise in widespread extreme rain events over central India. *Nat. Commun.* **2017**, *8*, 1–11. [CrossRef] [PubMed]
3. Kothawale, D.R.; Revadekar, J.V.; Kumar, K.R. Recent trends in pre-monsoon daily temperature extremes over India. *J. Earth Syst. Sci.* **2010**, *119*, 51–65. [CrossRef]
4. Kothawale, D.R.; Rupa Kumar, K. On the recent changes in surface temperature trends over India. *Geophys. Res. Lett.* **2005**, *32*, 1–4. [CrossRef]
5. Chandrashekhar, V. As the Monsoon and Climate Shift, India Faces Worsening Floods. Available online: https://e360.yale.edu/features/as-the-monsoon-and-climate-shift-india-faces-worsening-floods (accessed on 20 October 2020).
6. Azhar, G.S.; Mavalankar, D.; Nori-Sarma, A.; Rajiva, A.; Dutta, P.; Jaiswal, A.; Sheffield, P.; Knowlton, K.; Hess, J.J. Heat-related mortality in India: Excess all-cause mortality associated with the 2010 Ahmedabad heat wave. *PLoS ONE* **2014**, *9*. [CrossRef]
7. Times of India. Heat Waves Killed over 6000 since 2010. Available online: https://reliefweb.int/report/india/heat-waves-killed-over-6000-2010#:~{}:text=NEW%20DELHI%3A (accessed on 12 January 2020).

8. Rajsekhar, D.; Gorelick, S.M. Increasing drought in Jordan: Climate change and cascading Syrian land-use impacts on reducing transboundary flow. *Sci. Adv.* **2017**, *3*, 1–16. [CrossRef]
9. Herring, S.C.; Christidis, N.; Hoell, A.; Hoerling, M.P.; Stott, P.A. Explaining extreme events of 2017 from a climate perspective. *Bull. Am. Meteorol. Soc.* **2019**, *100*, S1–S117. [CrossRef]
10. Oueslati, B.; Yiou, P.; Jézéquel, A. Revisiting the dynamic and thermodynamic processes driving the record-breaking January 2014 precipitation in the southern UK. *Sci. Rep.* **2019**, *9*, 1–7. [CrossRef]
11. CarbonBrief Mapped: How Climate Change Affects Extreme Weather around the World. Available online: https://www.carbonbrief.org/mapped-how-climate-change-affects-extreme-weather-around-the-world (accessed on 10 April 2020).
12. Lawrence, D.M.; Hurtt, G.C.; Arneth, A.; Brovkin, V.; Calvin, K.V.; Jones, A.D.; Jones, C.D.; Lawrence, P.J.; De Noblet-Ducoudré, N.; Pongratz, J.; et al. The Land Use Model Intercomparison Project (LUMIP) contribution to CMIP6: Rationale and experimental design. *Geosci. Model Dev.* **2016**, *9*, 2973–2998. [CrossRef]
13. Sterling, S.M.; Ducharne, A.; Polcher, J. The impact of global land-cover change on the terrestrial water cycle. *Nat. Clim. Chang.* **2013**, *3*, 385–390. [CrossRef]
14. Thiery, W.; Visser, A.J.; Fischer, E.M.; Hauser, M.; Hirsch, A.L.; Lawrence, D.M.; Lejeune, Q.; Davin, E.L.; Seneviratne, S.I. Warming of hot extremes alleviated by expanding irrigation. *Nat. Commun.* **2020**, *11*, 1–7. [CrossRef]
15. Stoy, P.C. Deforestation intensifies hot days. *Nat. Clim. Chang.* **2018**, *8*, 360–369. [CrossRef]
16. Findell, K.L.; Berg, A.; Gentine, P.; Krasting, J.P.; Lintner, B.R.; Malyshev, S.; Santanello, J.A.; Shevliakova, E. The impact of anthropogenic land use and land cover change on regional climate extremes. *Nat. Commun.* **2017**, *8*, 1–9. [CrossRef]
17. Mueller, N.D.; Rhines, A.; Butler, E.E.; Ray, D.K.; Siebert, S.; Holbrook, N.M.; Huybers, P. Global relationships between cropland intensification and summer temperature extremes over the last 50 years. *J. Clim.* **2017**, *30*, 7505–7528. [CrossRef]
18. He, Y.; Lee, E.; Mankin, S.J. Seasonal tropospheric cooling in Northeast China associated with cropland expansion. *Environ. Res. Lett.* **2020**, *15*, 034032. [CrossRef]
19. Unnikrishnan, C.K.; Gharai, B.; Mohandas, S.; Mamgain, A.; Rajagopal, E.N.; Iyengar, G.R.; Rao, P.V.N. Recent changes on land use/land cover over Indian region and its impact on the weather prediction using Unified model. *Atmos. Sci. Lett.* **2016**, *17*, 294–300. [CrossRef]
20. Halder, S.; Saha, S.K.; Dirmeyer, P.A.; Chase, T.N.; Goswami, B.N. Investigating the impact of land-use land-cover change on Indian summer monsoon daily rainfall and temperature during 1951–2005 using a regional climate model. *Hydrol. Earth Syst. Sci.* **2016**, *20*, 1765–1784. [CrossRef]
21. Li, X.; Mitra, C.; Dong, L.; Yang, Q. Understanding land use change impacts on microclimate using Weather Research and Forecasting (WRF) model. *Phys. Chem. Earth* **2018**, *103*, 115–126. [CrossRef]
22. Gogoi, P.P.; Vinoj, V.; Swain, D.; Roberts, G.; Dash, J.; Tripathy, S. Land use and land cover change effect on surface temperature over Eastern India. *Sci. Rep.* **2019**, *9*, 1–10. [CrossRef]
23. Mukherjee, F.; Singh, D. Assessing Land Use–Land Cover Change and Its Impact on Land Surface Temperature Using LANDSAT Data: A Comparison of Two Urban Areas in India. *Earth Syst. Environ.* **2020**, *4*, 385–407. [CrossRef]
24. Nayak, S.; Mandal, M. Impact of land use and land cover changes on temperature trends over India. *Land Use Policy* **2019**, *89*. [CrossRef]
25. Lee, E.; Chase, T.N.; Rajagopalan, B.; Barry, R.; Biggs, T.; Lawrence, P. Effects of irrigation and vegetation activity on early Indian summer monsoon variability. *Int. J. Climatol.* **2009**, *29*, 573–581. [CrossRef]
26. Paul, S.; Ghosh, S.; Oglesby, R.; Pathak, A.; Chandrasekharan, A.; Ramsankaran, R. Weakening of Indian Summer Monsoon Rainfall due to Changes in Land Use Land Cover. *Sci. Rep.* **2016**, *6*, 1–10. [CrossRef] [PubMed]
27. Chen, L.; Dirmeyer, P.A. The relative importance among anthropogenic forcings of land use/land cover change in affecting temperature extremes. *Clim. Dyn.* **2019**, *52*, 2269–2285. [CrossRef]
28. Kang, S.; Eltahir, E.A.B. North China Plain threatened by deadly heatwaves due to climate change and irrigation. *Nat. Commun.* **2018**, *9*, 1–9. [CrossRef] [PubMed]
29. Sy, S.; Quesada, B. Anthropogenic land cover change impact on climate extremes during the 21st century. *Environ. Res. Lett.* **2020**, *15*. [CrossRef]
30. Christidis, N.; Stott, P.A.; Hegerl, G.C.; Betts, R.A. The role of land use change in the recent warming of daily extreme temperatures. *Geophys. Res. Lett.* **2013**, *40*, 589–594. [CrossRef]
31. Strack, J.E.; Pielke, R.A.; Steyaert, L.T.; Knox, R.G. Sensitivity of June near-surface temperatures and precipitation in the eastern United States to historical land cover changes since European settlement. *Water Resour. Res.* **2008**, *44*, 1–13. [CrossRef]
32. Wang, F.; Notaro, M.; Liu, Z.; Chen, G. Observed local and remote influences of vegetation on the atmosphere across North America using a model-validated statistical technique that first excludes oceanic forcings. *J. Clim.* **2014**, *27*, 362–382. [CrossRef]
33. He, Y.; Warner, T.A.; McNeil, B.E.; Lee, E. Reducing uncertainties in applying remotely sensed land use and land cover maps in land-atmosphere interaction: Identifying change in space and time. *Remote Sens.* **2018**, *10*, 506. [CrossRef]
34. Liu, H.; Gong, P.; Wang, J.; Clinton, N.; Bai, Y.; Liang, S. Annual dynamics of global land cover and its long-term changes from 1982 to 2015. *Earth Syst. Sci. Data* **2020**, *12*, 1217–1243. [CrossRef]
35. Van Etten, J.; Sumner, M.; Cheng, J.; Baston, D.; Bevan, A.; Bivand, R.; Busetto, L.; Canty, M.; Fasoli, B.; Forrest, D.; et al. Package 'Raster'. Available online: https://cran.r-project.org/web/packages/raster/raster.pdf (accessed on 8 October 2020).

36. Hersbach, H.; Bell, B.; Berrisford, P.; Hirahara, S.; Horányi, A.; Muñoz-Sabater, J.; Nicolas, J.; Peubey, C.; Radu, R.; Schepers, D.; et al. The ERA5 global reanalysis. *Q. J. R. Meteorol. Soc.* **2020**, *146*, 1999–2049. [CrossRef]
37. Santer, B.D.; Wigley, T.M.L.; Boyle, J.S.; Gaffen, D.J.; Hnilo, J.J.; Nychka, D.; Parker, D.E.; Taylor, K.E. Statistical significance of trends and trend differences in layer-average atmospheric temperature time series. *J. Geophys. Res. Atmos.* **2000**, *105*, 7337–7356. [CrossRef]
38. Gedney, N.; Valdes, P.J. The effect of Amazonian deforestation on the northern hemisphere circulation and climate. *Geophys. Res. Lett.* **2000**, *27*, 3053–3056.
39. Pal, S.; Ziaul, S. Detection of land use and land cover change and land surface temperature in English Bazar urban centre. *Egypt. J. Remote Sens. Sp. Sci.* **2017**, *20*, 125–145. [CrossRef]
40. Hurley, J.V.; Boos, W.R. Interannual variability of monsoon precipitation and local subcloud equivalent potential temperature. *J. Clim.* **2013**, *26*, 9507–9527. [CrossRef]
41. Ruxton, G.D. The unequal variance t-test is an underused alternative to Student's t-test and the Mann-Whitney U test. *Behav. Ecol.* **2006**, *17*, 688–690. [CrossRef]
42. Boschat, G.; Simmonds, I.; Purich, A.; Cowan, T.; Pezza, A.B. On the use of composite analyses to form physical hypotheses: An example from heat wave-SST associations. *Sci. Rep.* **2016**, *6*, 1–10. [CrossRef]
43. Roy, P.S.; Roy, A.; Joshi, P.K.; Kale, M.P.; Srivastava, V.K.; Srivastava, S.K.; Dwevidi, R.S.; Joshi, C.; Behera, M.D.; Meiyappan, P.; et al. Development of decadal (1985–1995–2005) land use and land cover database for India. *Remote Sens.* **2015**, *7*, 2401–2430. [CrossRef]
44. Duraisamy, V.; Bendapudi, R.; Jadhav, A. Identifying hotspots in land use land cover change and the drivers in a semi-arid region of India. *Environ. Monit. Assess.* **2018**, *190*. [CrossRef]
45. Tian, H.; Banger, K.; Bo, T.; Dadhwal, V.K. History of land use in India during 1880–2010: Large-scale land transformations reconstructed from satellite data and historical archives. *Glob. Planet. Chang.* **2014**, *121*, 78–88. [CrossRef]
46. Meiyappan, P.; Roy, P.S.; Sharma, Y.; Ramachandran, R.M.; Joshi, P.K.; DeFries, R.S.; Jain, A.K. Dynamics and determinants of land change in India: Integrating satellite data with village socioeconomics. *Reg. Environ. Chang.* **2017**, *17*, 753–766. [CrossRef]
47. Thiery, W.; Davin, E.L.; Lawrence, D.M.; Hirsch, A.L.; Hauser, M.; Seneviratne, S.I. Present-day irrigation mitigates heat extremes. *J. Geophys. Res.* **2017**, *122*, 1403–1422. [CrossRef]
48. Niu, X.; Tang, J.; Wang, S.; Fu, C. Impact of future land use and land cover change on temperature projections over East Asia. *Clim. Dyn.* **2019**, *52*, 6475–6490. [CrossRef]
49. Basha, G.; Kishore, P.; Ratnam, M.V.; Jayaraman, A.; Kouchak, A.A.; Ouarda, T.B.M.J.; Velicogna, I. Historical and Projected Surface Temperature over India during the 20th and 21st century. *Sci. Rep.* **2017**, *7*, 1–10. [CrossRef]
50. Chowdary, J.S.; John, N.; Gnanaseelan, C. Interannual variability of surface air-temperature over India: Impact of ENSO and Indian Ocean Sea surface temperature. *Int. J. Climatol.* **2014**, *34*, 416–429. [CrossRef]
51. Mishra, S.K.; Anand, A.; Fasullo, J.; Bhagat, S. Importance of the resolution of surface topography in Indian monsoon simulation. *J. Clim.* **2018**, *31*, 4879–4898. [CrossRef]
52. Kalsi, S.R.; Pareek, R.S. Hottest April of the 20th century over north-west and central India. *Curr. Sci.* **2001**, *80*, 867–873.
53. Brouwer, C.; Heibloem, M. Irrigation Water Management: Irrigation Water Needs. Available online: http://www.fao.org/3/s2022e/s2022e00.htm#Contents (accessed on 6 July 2020).
54. Kumar, M.D.; Sivamohan, M. Pampered Views and Parrot Talks: In the Cause of Well Irrigation in India. In Proceedings of the Sustaining Commons: Sustaining Our Future, the Thirteenth Biennial Conference of the International Association for the Study of the Commons, Hyderabad, India; 2011; pp. 1–24. Available online: https://dlc.dlib.indiana.edu/dlc/bitstream/handle/10535/7270/1205.pdf?sequence=1&isAllowed=y (accessed on 10 January 2021).
55. Chen, Y.; Niu, J.; Kang, S.; Zhang, X. Effects of irrigation on water and energy balances in the Heihe River basin using VIC model under different irrigation scenarios. *Sci. Total Environ.* **2018**, *645*, 1183–1193. [CrossRef] [PubMed]
56. Yang, Z.; Dominguez, F.; Zeng, X.; Hu, H.; Gupta, H.; Yang, B. Impact of irrigation over the California Central Valley on regional climate. *J. Hydrometeorol.* **2017**, *18*, 1341–1357. [CrossRef]
57. Ray, D.K.; Nair, U.S.; Welch, R.M.; Han, Q.; Zeng, J.; Su, W.; Kikuchi, T.; Lyons, T.J. Effects of land use in Southwest Australia: 1. Observations of cumulus cloudiness and energy fluxes. *J. Geophys. Res. Atmos.* **2003**, *108*, 1–20. [CrossRef]
58. Marcella, M.P.; Eltahir, E.A.B. Introducing an irrigation scheme to a regional climate model: A case study over West Africa. *J. Clim.* **2014**, *27*, 5708–5723. [CrossRef]
59. Stuart, E.A. Matching methods for causal inference: A review and a look forward. *Stat. Sci.* **2010**, *25*, 1–21. [CrossRef] [PubMed]